How to Cite:
Shamia, A. Y., Abd-Alhafez, A. A.-A., Zouair, M. G. A. (2022). Chemopreventive and therapeutic efficacy of thymoquinone on experimentally induced hamster buccal pouch carcinogenesis. *International Journal of Health Sciences*, *6*(S7), 2716–2734. https://doi.org/10.53730/ijhs.v6nS7.11937

Chemopreventive and therapeutic efficacy of thymoquinone on experimentally induced hamster buccal pouch carcinogenesis

Ashraf Yehia Shamia*
Assistant Lecturer, Oral and Dental Pathology Department, Faculty of Dental Medicine, Al-Azhar University, Palestine Tel.: *+2011131900*
*Correspondence email: dr_shamia@hotmail.com

Ahmed Abd-Alshakor Abd-Alhafez
Lecturer, Oral and Dental Pathology Department, Faculty of Dental Medicine (Boys- Cairo), Al-Azhar University, Egypt
Email: Dr.ahmedshokry1@gmail.com

Mohamed Gomaa Attia Zouair
Professor, Oral and Dental Pathology Department, Faculty of Dental Medicine (Boys-Cairo), Al-Azhar University, Egypt
Email: Dentistonline24@yahoo.com

***Abstract*---**Purpose: The present study aimed to investigate the chemopreventive and therapeutic effect of thymoquinone (TQ) on experimentally induced hamster buccal pouch carcinogenesis. Material: 40 Syrian male hamsters were classified into 4 equal groups (G(s)) of 10 each. GI: the animals remained untreated. The pouches of animals in GII, GIII, and GIV were painted 3 times a week for 14 weeks (ws) with 7,12-dimethylbenz (a) anthracene (DMBA). GII: no additional treatment was administered. Those in GIII: oral administration of TQ at a dose of 30 mg kg-1, one week before, as well as, during the application of DMBA on alternate days for 14 ws, whereas in GIV: the animals were injected intraperitoneally (IP) with TQ 50 mg/kg body weight thrice a week for 3ws. After the end of the experiment, the gross observations were made. Then, the fresh pouch specimens were surgically bisected into two pieces, one for hematoxylin and eosin (H&E) stain examination, measurement of the depth of invasion (DOI). The other piece was used for apoptosis detection through a flow cytometry (FCM) test. Results: gross observation showed variation in the reduction of the tumor size in GIII and GIV compared to GII. DOI revealed extremely significant difference (p value < 0.001) between GII either GIII or GIV. Regarding apoptosis results, there was highly significant difference (p value < 0.001) between either GI and GII, GII

and GIII, or GII and GIV. Conclusion: the TQ has a potential chemopreventive efficacy as well as a therapeutic promising outcome in regression of HBP carcinoma. Furthermore, TQ enhanced the apoptosis via downregulation of the Bcl-2 protein in HBP carcinoma.

***Keywords*---**TQ, apoptosis, Hamster buccal pouch (HBP) carcinoma.

Introduction

Oral squamous cell carcinoma (OSCC) has been responsible for more than 800.000 new cases and 450.000 deaths[1, 2]. 7,12-dimethylbenz (a) anthracene (DMBA) induced oral carcinogenesis in golden Syrian hamsters has become a well-accepted and well-characterized experimental paradigm for the investigation of biochemical, histological, and molecular alterations[3-15].

Regrettably, OSCC is linked with a high rate of morbidity and death, and despite significant progress in diagnosis and treatment options, the 5-year survival rate has not enhanced significantly, owing primarily to drug effectiveness issues, metastatic spread, and resistance[16, 17]. Nowadays, chemotherapy is still the most common treatment for OSCC[18]. Induction chemotherapy with cetuximab, carboplatin and paclitaxel are often used to treat OSCC[19-21]. However, these drugs develop acquired resistance and toxicity over time, leading to treatment limitations[22]. As a result, therapeutic approaches to tackle medication resistance and toxicity in OSCC patients are urgently required. Natural products, or their active constituents, are safe, affordable, and effective in treating various diseases, including cancer. Natural compounds are ubiquitously distributed throughout plants and marine organisms [23]. Chemoprevention is a promising approach to control, inhibit or suppress the tumor formation by using natural or synthetic entities, natural that possess antimutagenic, anticarcinogenic, antioxidant, anti-lipid peroxidative and anti-cell proliferating properties are considered as good chemopreventive agents in carcinogenesis including those of oral and experimental ones [6, 24-30]. A large number of phytochemicals ingested in human diet exhibit anticarcinogenic and antimutagenic effects(30). Thymoquinone (TQ) is a bioactive compound obtained from volatile oil of nigella sativa (NS). The NS was shown to contain about 24% TQ[13, 31-38]. Furthermore, several in vivo and in vitro studies have revealed the antineoplastic activities of TQ against a broad variety of

solid tumors including head and neck cancers, with few side effects[30, 39-43]. TQ is a pharmacologically active quinone, several studies were documented that TQ possess several medicinal properties including analgesic, anti-inflammatory, protective effect on lipid peroxidation and oxidative damage, anticonvulsant and also antioxidant effect[44-49]. Growth inhibition of TQ is associated with inhibition of DNA synthesis and induction of cell cycle arrest[50-56]. The present study was therefore designed to examine the effects of TQ on DMBA induced hamster buccal pouch (HBP) carcinogenesis. The evaluation depends on the histological tumor tissue changes and flow cytometry (FCM) investigations.

2. Material and Methods

2.1 Chemicals:

DMBA (0.5%) was gathered from Sigma-Aldrich company, solubilized in paraffin oil. TQ, also purchased from Sigma-Aldrich, and the olive oil was purchased from the local market. Stock solution of TQ (200mg/ml) was prepared in olive oil[57].

2.2 Animals:

Forty Syrian male hamsters, weighing between 80 and 120g, and 5 weeks (ws) old. The experimental hamsters were kept in standard boxes with sawdust bedding in a controlled environment with humidity (30-40%), temperature (20 ±2°C), and light (12-hour light/12-hour dark). A healthy hamster walks regularly and smoothly, had bright, clear eyes, healthy skin, and a soft, lustrous coat devoid of parasites, wounds, dry spots, and swellings.

2.3 Experimental design

The animals were randomly categorized into four group(s) (G(s)) after a week of adaptation. Each group had 10 animals. The right pouches of the animals in GII, GIII, and GIV were painted 3 times a week for 14 ws with 0.5% DMBA in liquid paraffin by a number 4 camel's hairbrush **(Fig. 1A). GII:** No additional treatment was given, while in **GIII** (chemoprevention G): TQ -DMBA, oral administration of TQ **(Fig.1B)** at a dose of 30 mg /1kg body weight, 1 week before, as well as, during the application of DMBA on alternate days for 14 ws[29]. Those in **GIV** (TQ G): The animals were injected IP by insulin syringe **(Fig.1C)** with TQ 50 mg/kg thrice a week for 3 ws[58].

2.4 General health examinations

The animal's general health was monitored throughout the experiment. Hamsters that demonstrated any of the following signs (crowding in sneezing, anorexia, silence, corner, diarrhea, discharge from the nose or eyes, dampness around the tail, wheezing, and hair loss) of illness or disease were adapted[4].

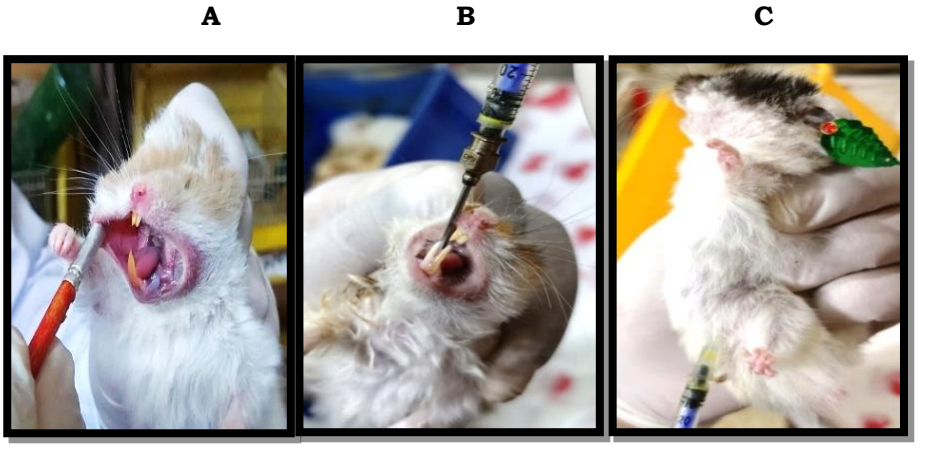

Fig. 1. Painting the HBP with DMBA **(A),** oral gavage **(B),** IP injection **(C)**

2.5 Gross observations and tumor volume measurement:

After termination of the experiment, gross observations of HBP mucosa were recorded (mucosal thickness, exudation, ulcers, and swelling). Then, the animals were euthanized, the right cheek pouch was everted, and the diameter of each tumor was measured with a Vernier calliper. The tumor volume, where the three diameters (mm) of the tumor are D1, D2 and D3, was calculated by the formula, Vmm3 = (4/3) π [(D1/2) (D2/2) (D3/2)][59].

2.6 Sample collection and preparation

The pouch on the right cheek was removed and bisected. For histological, one piece of fresh tissue was preserved in 10% neutral buffered formalin 24 houres, routinely processed, and preserved in paraffin blocks. The other fresh tissue sample was mechanically digested, immobilized, and subjected to FCM analysis.

2.7 Histopathological examinations

Utilizing a rotary microtome, 4 µm thick tissue sections were cut from the paraffin blocks, processed, mounted on glass slides, and stained with H&E for light microscopic examinations.

2.8 Measurement of the depth of invasion (DOI)

Using the H&E stained tissue sections, the DOI was calculated from the surface epithelium's basal layer to the deepest point of tumor infiltration. According to the American joint committee of cancer (AJCC), it is further characterized as less invasive at ≤5 mm, moderately invasive at 6-10 mm, and highly invasive at ≥10 mm [25]. The DOI was determined by a Leica QWIN V3 image analyzer computer system (Switzerland), which was operated via the Leica QWIN V3 software. This was done in Oral and Dental Pathology Department, Faculty of Dental Medicine (Boys-Cairo), Al-Azhar University, Egypt.

2.9. Flow cytometric analysis

2.9.1 Mechanical dissociation of the sample(60):

The tumor mass was placed into a 35 mm petri dish with 3 mL of PBS **(Fig.2A),** tumor specimen was extensively washed (2 to 3 times) in PBS to remove blood and debris. The specimen was held steady with tissue forceps, and with the back of a no. 22 scalpel blade, the specimen was scraped descending, and away, such that cells are go through the tumor mass into the dish **(Fig.2B,2C).** As cells were broken from the tumor mass, threads of connective tissue (C.T) were isolated, and were removed from the collection. The scrapping was continued until the tumor mass is too small to catch to have a large population in the dish. The tumor solution became pipetted up and down 3 to 5 min with a 5-ml disposable pipet. Then, the solution was placed into a 15-ml conical tube **(Fig.2D).** The remaining sample was centrifuged at 2500 rpm for 2 minutes at 4°C **(Fig.2E).** The media was aspirated off and the cellular pellet was resuspended in PBS in an appropriate volume needed for FCM analysis **(Fig.2F).**

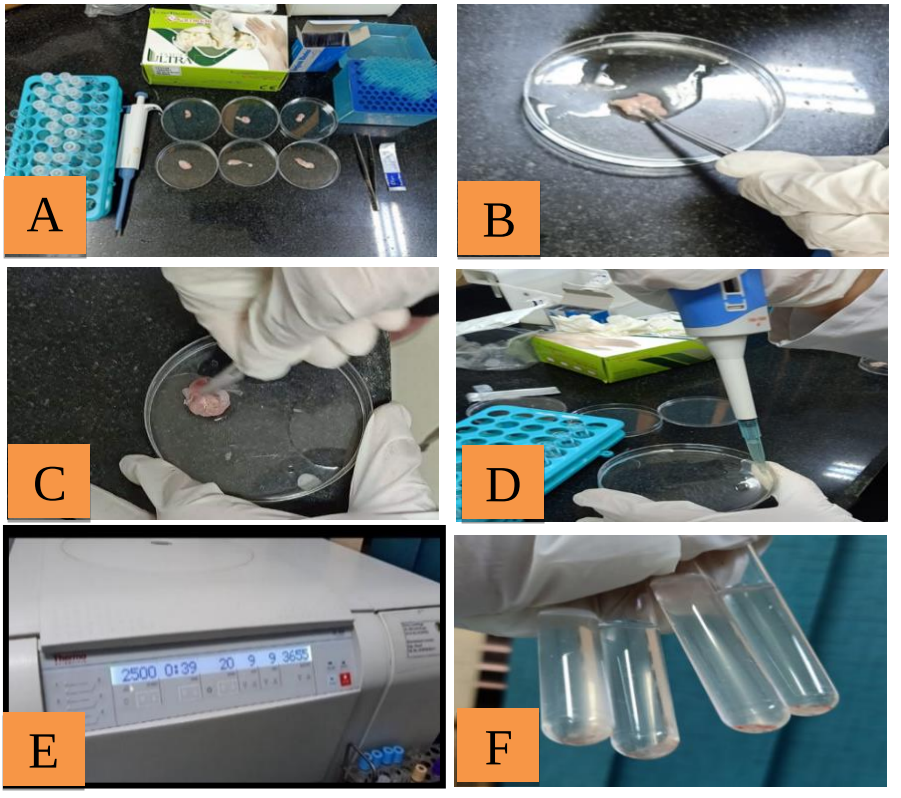

Fig. (2): Mechanical dissociation steps. Tumour mass in 35 mm petri dish **(A),** the specimen was held steady with tissue forceps **(B),** the specimen was scraped using the back of a no. 22 scalpel blade **(C),** the tumour solution was pipetted with a 5-ml disposable pipet (D), centrifuge machine (E) and the cellular pellet was resuspended in PBS **(F).**

2.10.2 Apoptosis assay of all specimen cells:

Annexin V/ Propidium iodide (PI) apoptosis detection kit was used. The cells were washed and placed in 100 µL of the annexin V-conjugate binding buffer to which 10 µL of FITC-conjugated Annexin and 10 µl of PI were added. After incubation for 15 min, 400 µL of the binding buffer was added. Cells were analysed by the usage of a flow cytometer (BD FACSCalibur, San Jose, CA, USA) with BD FACSDiva 7.0 software **(Fig.3A).** This was done by finical support in the FCM Unit, Clinical Pathology Department, South Egypt Cancer Institute, Assiut University, Egypt. Many thanks to Dr. Asmaa Mohamed Zahran Omar Professor, Department of Clinical pathology South Egypt Cancer Institute Assiut University for her efforts to performed various procedures.

The profile graph, presented the Annexin V FITC parameter along the X-axis and the PI parameter along the Y-axis. Four different populations of cells were distinguished, in a clockwise direction starting from the upper left quadrant: cells that were stained with PI (necrotic), those that have both bound to annexin-V FITC and been labelled with PI (late apoptotic), and those that have bound to annexin-V FITC only (early apoptotic), those that have been unlabelled (viable cells). Of these four kinds of cell modes, early and late apoptosis were calculated among the cell population **(Fig.3B).**

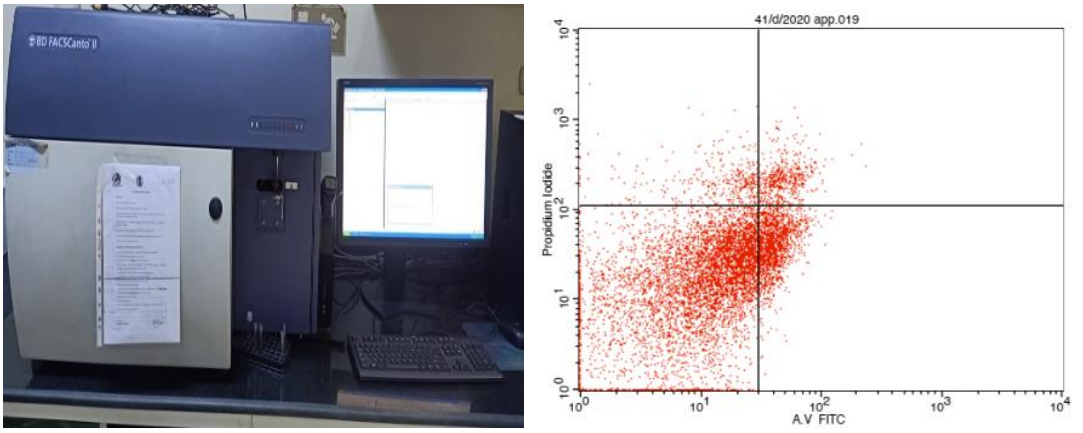

Fig. (3): FACS Calibur flow cytometer (BD Biosciences) with Cell Quest software **(A),** apoptosis assay profile graph **(B).**

2.10 Statistical analysis

The data were statistically examined, and the mean and standard deviation (SD) were calculated. A one-way analysis of variance was performed using SPSS version 17.0 for Windows (ANOVA). With quantitative data and parametric distribution, ANOVA was utilized to differentiate between more than two separate groups, accompanied by post hoc analysis with the least significant difference LSD test. To establish significance, the relevant p-values were used: p 0.05: significant, p > 0.05: non-significant, and p< 0.001: highly significant.

3. Results

3.1.Gross observations

GI examination revealed no obvious alterations, neither hair loss or skin ulcerations. The HBP was normal pale pink with no pathological or inflammatory signs **(Fig. 4A),** the hamasters buccal pouch length was (5-5.5) cm. Those in **GII** demonstrated debilitation and observable hair loss with para-oral skin ulcerations. Large exophytic growths with prominent vascularity in the animals' pouches, in addition to eroded, and ulcerative areas with spontaneous bleeding were seen **(Fig. 4B).** The mean tumors volume measurement of tumor-bearing animals in ten hamesters in **GII** was 814.6 mm3 (620 – 1005 mm3), and the pouch length in **GII** recorded (1.5-2 cm). **GIII** revealed no observable abnormalities except redness at the painting site **(Fig. 4C),** while **GIV** showed slight improvement in the general health compared to the animals in **GII,** Perioral skin ulcers and hair loss were seen, other areas showed small exophytic nodule with an absence of ulceration and bleeding **(Fig. 4D).** The pouch length in GIII recorded from 4- 4.5 cm and in GIV was 3-3.5cm. There was high significant difference (p value <0.001) in pouch length between GI and either **GII** or **GIV,** while **GI** and **GIII** recorded significant difference (p value = 0.036). The mean tumors volume measurement in those of **GIII** and **GIV** was 22.15 mm3 (17.5 – 28.1mm3) and 269.13 mm3 (230.4 – 310.2 mm3), respectively. There was highly significant difference (p value < 0.001) in tumor volume either GIII or GIV Comparing the GII.

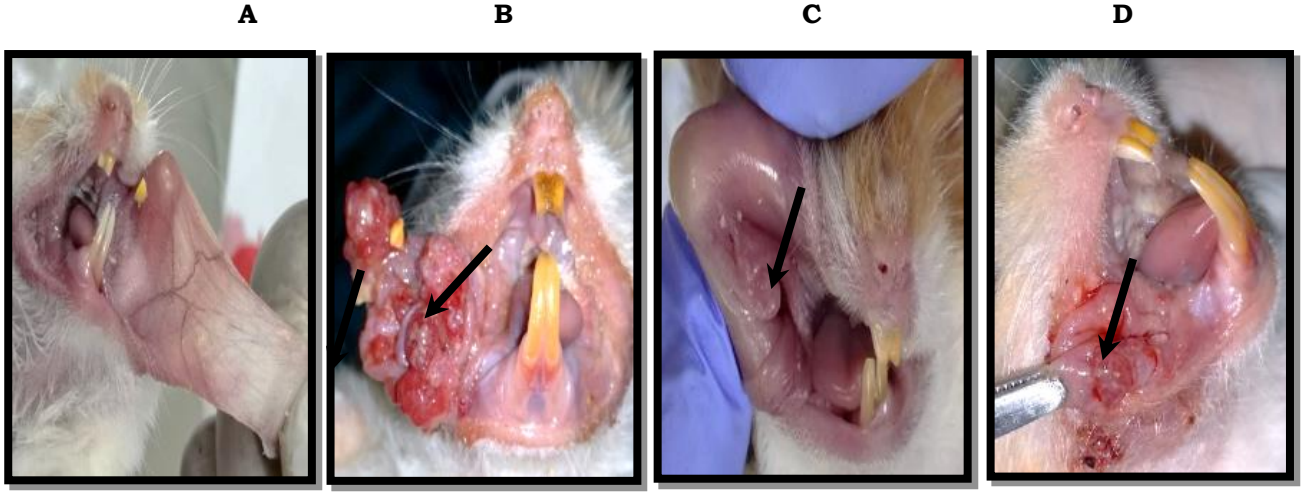

Fig. 4. (A) GI's HBP indicates normal buccal pouch mucosa, which appeared pink in colour with a smooth surface **(B).** GII's HBP demonstrates multiple exophytic papillary tumour masses surrounded by bleeding areas **(C).** GIII's HBP showing small exophytic nodule with absence of ulceration and bleeding **(D).** GIV's HBP indicates a small size nodule with little bleeding areas (arrow).

3.2. Histological, DOI findings:

HBP mucosa, using H&E stain, in **GI,** exhibited normal thin stratified squamous epithelium with minor keratinization, consisting of 2-4 layers of squamous cells. A subepithelial connective tissue, a muscle layer and an areolar connective tissue were seen **(Fig.5A).** HBP mucosa, using H&E stain, in **GII**, the overlying epithelium revealed different degrees of epithelial dysplasia with true invasion. Areas of the overlying epithelium exhibited papillomatous presentations, multiple areas with dysplastic features including basal cell hyperplasia, loss of polarity, hyperchromatism, prominent nucleoli, altered N\C ratio, swirling of spinous layer and cellular & nuclear pleomorphism (**Fig.5B)**. Destruction n of the basement membrane with true invasion of malignant cells (well differentiated and moderately differentiated SCC) with different degrees penetration into the underlying CT, with intense marked chronic inflammatory cells were seen (**Fig.5C)**. The mean DOI in GII (10 hamsters) was 10.5mm (**Fig.5D)**. HBP mucosa in **GIII** revealed the overlying epithelium with various finding, although areas with almost normal features, in 7out of 10 hamsters, the overlying epithelium exhibited different degrees of epithelial dysplasia without true invasion. 2 hamsters with moderate epithelial dysplastic features occupying the two-third of the epithelium thickness were seen. These included hyperchromatism, altered N\C ratio, swirling of spinous layer and abnormal mitosis, 3 displayed severe epithelial dysplasia with dysplastic features extended to more than two-thirds of the epithelial thickness **(Fig. 5E)**. 2 hamsters displayed carcinoma in situ (CIS) with dysplastic features affecting the entire epithelium thickness in addition to basillar hyperplasia. In the last 3 hamsters, the dysplastic overlying epithelium was accompanied by destruction of the basement membrane. The underlying CT showed superficial invasion of the malignant cells and keratin pearl formations in the form of well differentiated SCC that extended into the subepithelial connective tissue. The last showed intense inflammatory cell infiltration and collagen fibres surrounding the invasive nests with limited necrosis **(Fig.5F).** With mean DOI = 0.8mm**.** HBP mucosa in **GIV**, 5 out of 10 hamsters, exhibited different degrees of epithelial dysplasia: 2 with severe dysplasia and 3 with CIS showed hyperchromatism, changed N/C ratio, conspicuous nucleoli, cellular & nuclear pleomorphism, and keratin pearls within the epithelial layer. The remaining 5 animals exhibited true invasion, well-differentiated SCC within the connective tissue that showed island of dysplastic epithelium surrounded by fibrosis, was seen **(Fig.5G),** with mean DOI = 2.4mm. An intense inflammatory infiltrate and muscle tissue with almost regular pattern and thickness were noticed.

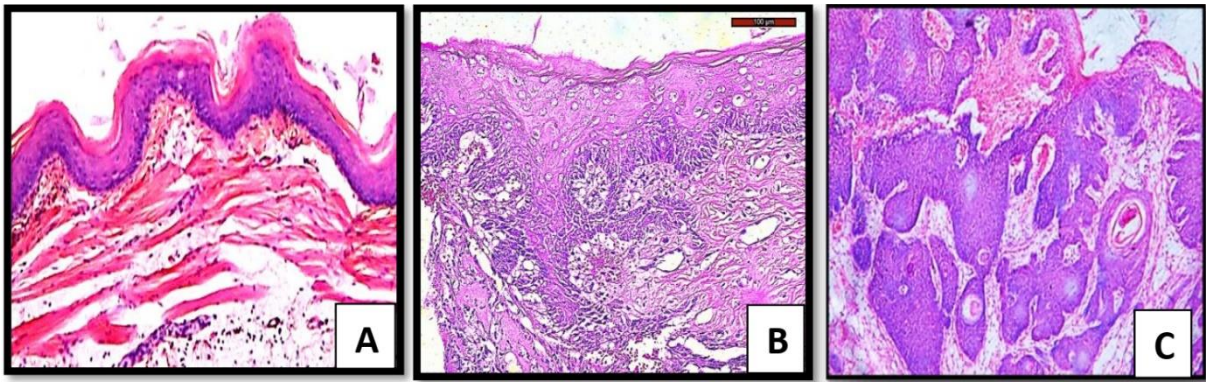

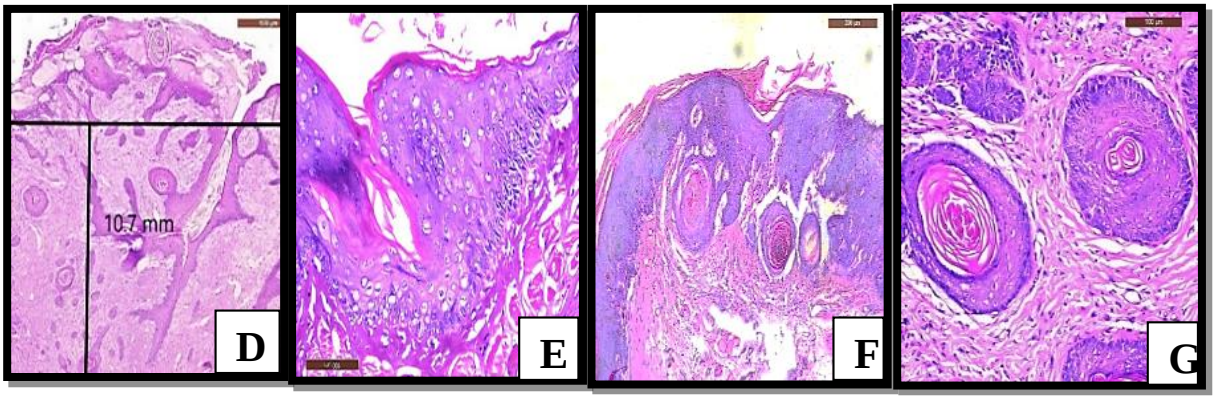

Fig. 5A. H&E stain demonstrates two to four layers of epithelium, superficial keratinized squamous cells, connective tissue layer, flattened rete ridges, muscular layer, and deep layer of loose areolar connective tissue. **5B.** shows basal cell hyperplasia, loss of polarity, hyperchromatism, prominent nucleoli and cellular & nuclear pleomorphism **5C.** shows well-differentiated SCC with deep penetration of several tumour islands into the underlying connective tissue and sub-epithelial inflammatory infiltrates. **5D.** Photograph of measuring the DOI, the greatest invasion was measured by dropping a "plumb line" from the horizon to the deepest invasive cancer cells. **5E** shows severe dysplasia with dysplastic feature. **5F.** reveals well differentiated SCC (superficial invasion). **5G.** reveals true invasion, well-differentiated SCC within the connective tissue that showed areas of fibrosis, but not in the muscular layer.

3.3. Detection of apoptosis by flow cytometry:

With regard to apoptosis of all specimen cells, in the untreated cells (normal control), 1.83% of the cells underwent apoptosis, while the cells in DMBA group **GII** resulted in 23.7% apoptosis. In the study groups, TQ chemopreventive **GIII** resulted in 71.3% apoptosis, while treatment with TQ in **GIV** resulted in 53.7% apoptosis. There was highly significant difference (p value < 0.001) between either GI and GII, GII and GIII, or GII and GIV, **table (1), chart (1).**

Table (1): Comparison between the studied groups regarding apoptosis of cancer cells (%)

	Apoptosis of cancer cells%					
	Mean ± SD	**Range**	**G1**	**GII**	**GIII**	**GIV**
GI	1.83 ± 0.51	0.9 – 2.7	--	0.000	0.000	0.000
GII	23.70 ± 4.88	16.8 – 33.4	0.000	--	0.000	0.000
GIII	71.30 ± 12.74	55.7 – 88.3	0.000	0.000	--	0.000
GIV	53.70 ± 10.91	33.8 – 74.1	0.000	0.000	0.000	--
F	**66.936**					
P-valu	**<0.001 (HS)**					

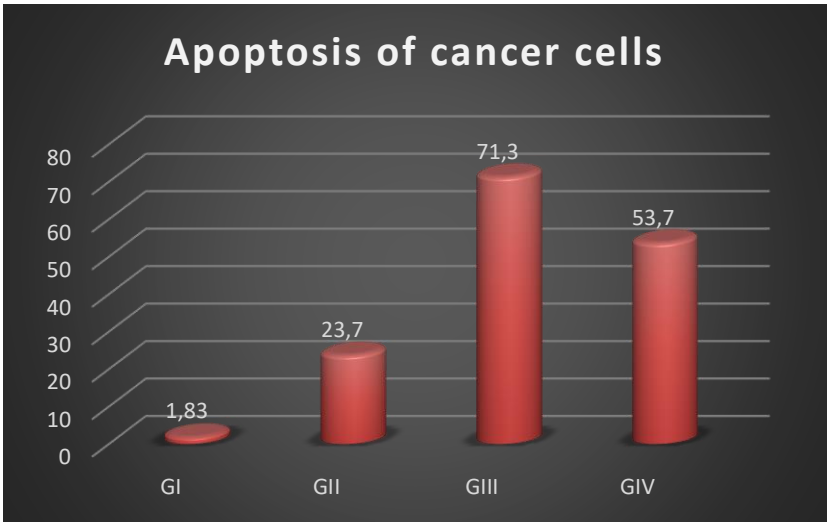

Chart (1): Comparison between the studied groups regarding apoptosis of cancer cells (%).

Correlation analysis of FCM apoptosis with tumor volume and DOI, among the studied group: (Table:3)

In summary, there was statistically significant (p-value = 0.000) negative correlation of FCM apoptosis with tumor volume and depth of invasion. This means that an increase in one variable is associated with a decrease in the other variable and vice versa.

Table (2):

	FCM apoptosis	
	R	**p-value**
Tumor volume	**-0.876****	**0.000**
DOI	**-0.493****	**0.000**

4. Discussion

Oral cancer is one of the most disfiguring kinds of cancer. Despite the significant advancement in oral cancer treatment strategy, it remains a major induction of morbidity in human populations. In the present study, using the hamster cheek pouch system of the oral carcinogenesis model reflected the beneficial for a deeper understanding of cancer biology, prevention, and treatment. These was done by gross observation, DIO by H&E stain and apoptosis by FCM results during

carcinoma induction as well as when utilizing thymoquinone as chemopreverntive or therapeutic treatment.

In the present study, GII revealed noticeable systemic debilitation in all animals, in addition to perioral alteration and HBP tumor growth compared to GI. The latter was distinguishable by the results of the volume of tumor-bearing pattern (620 – 1005 mm3). Also, a decrease in the pouch length in GII (1.5-2 cm) compared to that of GI (5 cm) due to necrosis in the distal end of the pouch. Generally speaking, The results in GII are in consistence with those reported by other investigators [11, 28] These observations are mainly due to the strong toxic DMBA effect.

In the present study, GIII showed obviously improvement in the animal's general health and active throughout the experimental period and the pouch length in GIII recorded from (4- 4.5 cm), was increased compared to GII (1.5-2cm), furthermore, the mean tumor volume measurement in GIII was (22.15 mm^3) which is statistically high significant difference (p value < 0.001) compared to GII. These findings were in agreement with other studies[30, 33]. Rajkamal et al (2010)[29] study indicates that TQ has potent chemopreventive efficacy in experimental oral carcinogenesis. Oral administration of TQ to DMBA painted hamsters significantly normalized and inhibited the abnormalities seen in cell surface glycoconjugates in the tumor tissues and circulation during carcinogenesis, and restored the expression of cytokeratin, which indicates their membrane stabilizing effect of TQ during neoplastic transformation. The protective role of TQ is probably due to their inhibitory role on glycoprotein synthesis or on the activity of the glycosyl transferase. Chemoprevention role of TQ involves its inhibition of the tumorigenic generation of superoxide anions and nitric oxide as well as its role as a scavenger of carcinogenic free radicals[30].

In the present study GIV showed a relatively slight improvement in the animal's general health, decrease in size of the papillomatous lesions was observed. The pouch length in GIV recorded from (3- 3.5 cm), was increased compared to GII (1.5-2cm), furthermore, the mean tumor volume measurement in GIV was (269.13 mm^3) which is statistically high significant difference (p value < 0.001) compared to GII... They were in line with another study Majdalawieh et al (2017)[32].

In the present study, the histopathological findings, using H&E stain, GII revealed a development of diverse patterns of invasive SCC (50 % well-differentiated and 50 % moderately differentiated) that expanded into deeper areas of connective tissue (C.T) (DOI=10.5mm). These results are in line with previous studies[5, 6, 22]. This could be due to proclivity for carcinogenesis since it is metabolized by phase I enzymes such as cytochrome P450 to its final carcinogenic metabolite, dihydrodiol epoxide, which damages DNA, this in turn causing mutation and cancer[4]. Furthermore, ROS has been implicated throughout phases of carcinogenesis (promotion, initiation, and progression). ROS can cause DNA damage, proto-oncogenes stimulation, tumor suppressor genes suppression, all of which can lead to neoplastic transformation[12]. Contrastingly, in the study conducted by Hussein et al

(2018)[21] only 66.67% of the hamsters developed oral tumors, and that could be attributed to the different solvent material.

The histopathological findings in GIII revealed variable changes, range: hyperkeratosis, hyperkeratosis and focal hyperplasia, mild dysplasia and well differentiated SCC with superficial invasion of tumor cells not extended to the deeper areas (the mean DOI=0.8mm). This reflected highly significant difference (p-value <0.001) compared to GII. These results are in line with another study Swidan et al (2016) [26].

The histopathological findings in GIV revealed variable changes, range: severe dysplasia to less invasive well differentiated SCC, not extended to deeper areas (DOI=2.4mm) which had high significance difference (p value <0.001) between GIV and GII. This due to therapeutic efficacy of TQ. Also, its effect on muscular layer through muscle tissue pattern with an elevation in the thickness of the striated muscle layer. At the same time, a few tumor masses were substituted by proliferating fibrous tissue with enhanced collagen deposition. The latter is with aline with Amer et al (2020)[27] study, explained that, TQ could be internalized into malignant cells and thus induce its full activities.

In the present study, FCM of apoptosis results in GII revealed only 23.7% undergo apoptosis of highly proliferative cancer tissue compared to GI 1.83% this was reflected by the highly significant difference (p value < 0.001). DMBA have a stimulatory effect on Bcl-2 which makes the removal of genetically modified cells difficult, fevering the accumulation of new mutations, which can result in the appearance of cells with malignant phenotype. These results are in agreement with other studies[14, 15]. Mariadoss et al (2019)[9], whom stated that, Bcl-2 has the capacity of interrupting the apoptosis process both in the initial and final phases because this protein stabilizes the potential of the mitochondria membrane when forming heterodimers with Bax.

In the current study, FCM of apoptosis results in GIII revealed that, highly significant difference (p value < 0.001) between GIII and GII. These results are in agreement with Malik et al (2021)[36]. Hussain et al (2011)[41] revealed that, TQ-induced ROS generation is involved in promoting apoptosis in primary effusion lymphoma cells by inhibiting AKT.

Furthermore, FCM of apoptosis results in GIV revealed that, high significant difference (p value <0.001) between GIV and either GII or GIII. This result is in agreement with those of other investigators[13, 17, 37]. TQ can also plays its anti-cancer effect by modulate tumor suppressor genes such as P53, P21 and P27. TQ can induce cancer cell apoptosis by decreasing Bcl-2 and increasing Bax and increasing the release of cytochrome C. TQ can also cause the apoptosis in gastric carcinoma by initiating the activation of caspase-3 and caspase-9[38, 57].

Conclusion:

In conclusion, this study realized a potential chemopreventive efficacy as well as a therapeutic promising outcome of TQ in regression of HBP carcinoma model, not only in gross observation results, but also, in tumor volume, histopathological,

DOI and apoptosis assay results. The TQ has a potential chemopreventive efficacy as well as a therapeutic promising outcome in regression of HBP carcinoma. Furthermore, TQ enhanced the apoptosis via downregulation of the Bcl-2 protein in HBP carcinoma. Accordingly, we recommend combination of TQ as prophylactic and therapeutic use in the same model. in clinical trials with further research studies in order to evaluate the clinical efficacy of TQ alone and in combination with other chemotherapeutic drugs to continue the limited positive results concerning chemotherapy.

CRediT authorship contribution statement: Mohamed Gomaa Attia Zouair: Conceptualization, Methodology, Investigation, Formal analysis, Writing original draft. **Ahmed Abd-Alshakor Abd-Alhafez**: Supervision, Investigation, Funding acquisition. **Ashraf Yehia Shamia**: Conceptualization, Funding acquisition, Resources, Supervision, Writing – review & editing.

Conflicts of interests: The authors declare no conflicting financial interests.

Data Availability: The Data presented in this study are available on request from the corresponding author.

Funding: This research did not receive any specific grant from funding agencies in the public, commercial, or not-for-profit sectors.

Institutional review board statement

The National Research Council's Guide for the Care and Use of Laboratory Animals have been followed. All experiments were approved by ethical committee of Faculty of Dental Medicine (Boys Cairo), Al-Azhar University, Egypt (Ethical Code No. 489/2302).

Reference

1. Ma H, Liu C, Zhang S, Yuan W, Hu J, Huang D, et al. miR-328-3p promotes migration and invasion by targeting H2AFX in head and neck squamous cell carcinoma. Journal of Cancer. 2021;12(21):6519.
2. Zawam HH, Selim A, Osman NO, Edesa W. Factors Influencing the Response Rateand Survival of Testicular Germ Cell Tumors: A Single Institution Experience from Egypt. Research in Oncology. 2021;17(2):66-72.
3. Balakrishnan V, Ganapathy S, Veerasamy V, Duraisamy R, Sathiavakoo VA, Krishnamoorthy V, et al. Anticancer and antioxidant profiling effects of Nerolidol against DMBA induced oral experimental carcinogenesis. Journal of Biochemical and Molecular Toxicology. 2022:e23029.
4. Elagouz M, alhafez A, Zahran A, Zouair M. Flow cytometric assessment of nivolumab and/or epigallocatechin-3-gallate on cancer stem cells of DMBA induced hamster buccal pouch carcinoma. Medical Science. 2022;25:3206-21.
5. Vijayalakshmi S, Mariadoss AVA, Ramachandran V, Shalini V, Agilan B, Sangeetha CC, et al. Polydatin encapsulated poly [lactic-co-glycolic acid] nanoformulation counteract the 7, 12-dimethylbenz [a] anthracene mediated

experimental carcinogenesis through the inhibition of cell proliferation. Antioxidants2019;8(9):375.
6. Selvasundaram R, Manoharan S, Buddhan R, Neelakandan M, Murali Naidu. Chemopreventive potential of esculetin in 7, 12-dimethylbenz (a) anthracene-induced hamster buccal pouch carcinogenesis. Molecular Cell Biochemistry 2018;448(1):145-53.
7. Rajasekaran D, Manoharan S, Silvan S, Vasudevana K, Baskaran N, Palanimuthu. Proapoptotic, anti-cell proliferative, anti-inflammatory and antiangiogenic potential of carnosic acid during 7, 12 dimethylbenz [a] anthracene-induced hamster buccal pouch carcinogenesis. African Trade Complement Altern Medicine 2013;10(1):102-12.
8. M Mohamed A, M Mansour. Effect of oxygenated water as a new chemopreventive modality in experimentally induced hamster buccal pouch carcinogenesis. Al-Azhar Journal of Dental Science 2018;21(2):99-112.
9. Mariadoss AVA, Vinayagam R, Xu B, Venkatachalam K, Sankaran V, Vijayakumar S, et al. Phloretin loaded chitosan nanoparticles enhance the antioxidants and apoptotic mechanisms in DMBA induced experimental carcinogenesis. Chemical Biological Interaction2019;308:11-9.
10. Alqalshy EM, Ibrahim AM, Abdel-Hafiz AA-S, Kamal KAE-R, Alazzazi MA, Omar MR, et al. Effect of docosahexaenoic acid as a chemopreventive agent on experimentally induced hamster buccal pouch carcinogenesis. Cancer Tratment and Research Communications 2022;31:100558.
11. Bruna F, Arango-Rodríguez M, Plaza A, Espinoza I, Conget P. The administration of multipotent stromal cells at precancerous stage precludes tumor growth and epithelial dedifferentiation of oral squamous cell carcinoma. Stem Cell Journal. 2017;18:5-13.
12. Naveenkumar C, Raghunandhakumar S, Asokkumar S, Devaki T. Baicalein abrogates reactive oxygen species (ROS)- mediated mitochondrial dysfunction during experimental pulmonary carcinogenesis in vivo. Basic Clinical Pharmacology Toxicology 2013;112(4):270-81.
13. Rukoyatkina N, Butt E, Subramanian H, Nikolaev VO, Mindukshev I, Walter U, et al. Protein kinase A activation by the anti-cancer drugs ABT-737 and thymoquinone is caspase-3-dependent and correlates with platelet inhibition and apoptosis. Cell Death & Disease.2017;8(6):e2898-e.
14. Hussein AM, El-Sheikh SM, Attia MA, Ramadan OR, Omar EM. Analysis of DNA ploidy and S-phase fraction in relation to development of oral squamous cell carcinoma: an experimental study. Oral Medicine, X-Ray, Oral Biology and Oral Pathology: 2019;65(3):2447-55.
15. Ramachandhiran D, Vinothkumar V, Babukumar S. Paeonol exhibits anti-tumor effects by apoptotic and anti-inflammatory activities in 7, 12-dimethylbenz (a) anthracene induced oral carcinogenesis. Biotechnology Histochemistry. 2019;94(1):10-25.
16. Yanamoto S, Umeda M, Kioi M, Kirita T, Yamashita T, Hiratsuka H, et al. Multicenter retrospective study of cetuximab plus platinum-based

chemotherapy for recurrent or metastatic oral squamous cell carcinoma. Cancer Chemotherapy and Pharmacology. 2018;81(3):549-54.
17. Saleh MM, Darwish ZE, El Nouaem MI, Mourad GM, Ramadan. Chemopreventive effect of green tea and curcumin in induced oral squamous cell carcinoma: An experimental study. Alexandria Dental Journal. 2020;45(3):74-80.
18. Wang X, Li N, Meng J, Wen N. The use of topical ALA-photodynamic therapy combined with induction chemotherapy for locally advanced oral squamous cell carcinoma. American Journal of Otolaryngology. 2021;42(6):103112.
19. Liu B, Cao G, Dong Z, Guo T. Effect of microRNA-27b on cisplatin chemotherapy sensitivity of oral squamous cell carcinoma via FZD7 signaling pathway. Oncology Letters.2019;18(1):667-73.
20. Bauman J, Langer C, Quon H, Algazy K, Lin A, Desai A, et al. Induction chemotherapy with cetuximab, carboplatin and paclitaxel for the treatment of locally advanced squamous cell carcinoma of the head and neck. Experimental Therapeutic Medicine.2013;5(4):1247-53.
21. Hussein AM, El-Sheikh SM, Darwish ZE, Hussein KA, Gaafar A. Effect of genistein and oxaliplatin on cancer stem cells in oral squamous cell carcinoma: an experimental study. Alexandria Dental Journal.2018;43(1):117-23.
22. Shamia AYM, Abd-Alhafez A-A, Al-qalshy ES, Zouair MGA. Therapeutic efficacy of time-dependent cetuximab on experimentally induced hamster buccal pouch carcinoma. International Journal of Health Sciences. 2022;6(S5):3431-56.
23. Rahmani AH, Aly S. Nigella sativa and its active constituents thymoquinone shows pivotal role in the diseases prevention and treatment. Asian Journal Pharmacological Clinical Resarch 2015;8(1):48-53.
24. AlAttas SA, Fat'heya MZ, Turkistany S. Nigella sativa and its active constituent
thymoquinone in oral health. Saudi Medical Journal. 2016;37(3):235.
25. El-Hossary WH, Hegazy E, El-Mansy M. Topical chemopreventive effect of thymoquinone versus thymoquinone loaded on gold nanoparticles on DMBA-induced hamster buccal pouch carcinogenesis. Oral Medicine, X-Ray, Oral Biology and Oral Pathology. 2018;64(4) 3523-33.
26. Swidan S, Hassan M, El-Hossary W. Chemopreventive effect of different doses of nanothymoquinone on chemically–induced oral carcinogenesis: Oral Medicine, X-Ray, Oral Biology and Oral Pathology. 2021;67(8):3157 3169.
27. Amer MH, Hassan MMA, Attia FM, El-nour A, Mohamed K, Korraah A. XRCC1 immunohistochemical expression in DMBA–induced oral squamous cell carcinoma treated with different thymoquinone preparations. Dental Journal of Suez Canal University 2020;1(2):151-9.

28. Casto BC, Knobloch TJ, Galioto RL, Yu Z, Accurso BT, Warner B. Chemoprevention of oral cancer by lyophilized strawberries. Anticancer Resarch
2013;33(11):4757-66.
29. Rajkamal G, Suresh K, Sugunadevi G, Vijayaanand M, Rajalingam K. Evaluation of chemopreventive effects of Thymoquinone on cell surface glycoconjugates and cytokeratin expression during DMBA induced hamster buccal pouch carcinogenesis.BMB Rep2010;43(10):664-9.
30. Gomathinayagam R, Ha JH, Jayaraman M, Song YS, Isidoro C, Dhanasekaran D. Chemopreventive and anticancer effects of thymoquinone: Cellular and Molecular Targets. 2020;25(3):136.
31. Atta M. Some characteristics of nigella (Nigella sativa L.) seed cultivated in Egypt and its lipid profile. Food Chemistry 2003;83(1):63-8.
32. Majdalawieh AF, Fayyad MW, Nasrallah G, nutrition. Anti-cancer properties and mechanisms of action of thymoquinone, the major active ingredient of Nigella sativa. Food Science and Nutrition 2017;57(18):3911-28.
33. Algharyni HM, El-Hossary WH, Korraah AM, Hassan MM. Expression of myod in the dmba-treated hamster pouches following thymoquinone injection: IOSR Journal of Dental and Medical Sciences 2019;18(2):35-40.
34. Tabassum S, Thakur V, Rosli N, Ichwan SJA, Mishra P, Suriyah W. Therapeutic implications of thymoquinone and its molecular and functional mechanisms against oral and lung cancer. Pharmaceuticals Journal. 2022;15(3)23-44.
35. Imran M, Rauf A, Khan IA, Shahbaz M, Qaisrani TB, Fatmawati S, et al. Thymoquinone: A novel strategy to combat cancer: Biomedicine & Pharmacotherapy. 2018;106:390-402.
36. Malik S, Singh A, Negi P, Kapoor V. Thymoquinone: A small molecule from nature with high therapeutic potential. Drug Discovery Today. 2021;26(11):2716-25.
37. El-Wahed A, Asmaa M, Hassan MM, El-Hossary WH, Korraah A. Localization of cyclooxygenase-2 in experimentally–induced carcinogenesis following treatment with thymoquinone loaded on nano-gold particles. Alexandria Dental Journal 2018;43(3):81-7.
38. Said R. Early Thymoquinone Injections and Expression of DNA Repair Enzymes in Hamster Buccal Pouch-Induced Dysplasia. Egypt Dental Journal 2021;67(4):3157-69.
39. Schneider-Stock R, Fakhoury IH, Zaki AM, El-Baba CO, Gali-Muhtasib H. Thymoquinone: fifty years of success in the battle against cancer models. Drug Discovery Today2014;19(1):18-30.
40. Helmy SA, El-Mesery M, El-Karef A, Eissa LA, El Gayar A. Thymoquinone upregulates TRAIL/TRAILR2 expression and attenuates hepatocellular carcinoma in vivo model. Life Sciences 2019;233:116673.
41. Hussain AR, Ahmed M, Ahmed S, Manogaran P, Platanias LC, Alvi SN, et al. Thymoquinone suppresses growth and induces apoptosis via generation of

reactive oxygen species in primary effusion lymphoma. Free Radical Biology and Medicine 2011;50(8):978-87.
42. Kotowski U, Heiduschka G, Kadletz L, Fahim T, Seemann R, Schmid R, et al. Effect of thymoquinone on head and neck squamous cell carcinoma cells in vitro: Synergism with radiation. Oncology Letters 2017;14(1):1147-51.
43. Woo CC, Loo SY, Gee V, Yap CW, Sethi G, Kumar AP, et al. Anticancer activity of thymoquinone in breast cancer cells: possible involvement of PPAR-γ pathway. Biochemical Pharmacology 2011;82(5):464-75.
44. Phua CYH, Teoh ZL, Goh B-H, Yap WH, Tang Y. Triangulating the pharmacological properties of thymoquinone in regulating reactive oxygen species,
inflammation, and cancer: Therapeutic applications and mechanistic pathways. Life Sciences 2021;287:120120.
45. Ibrahim S, Fahim SA, Tadros SA, Badary O. Suppressive effects of thymoquinone on the initiation stage of diethylnitrosamine hepatocarcinogenesis in rats. Journal of Biochemical and Molecular Toxicology 2022:e23078.
46. Boskabady MH, Saadat S, Ghorani V. Experimental and Clinical Studies on the Effects of Nigella Sativa and its Constituents on Allergic and Immunological Disorders. Phytotherapy Research 2022;5:121.
47. Koka PS, Mondal D, Schultz M, Abdel-Mageed AB, Agrawal K. Studies on molecular mechanisms of growth inhibitory effects of thymoquinone against prostate cancer cells: role of reactive oxygen species. Experimental Biological Medicine 2010;235(6):751-60.
48. Relles D, Chipitsyna GI, Gong Q, Yeo CJ, Arafat H. Thymoquinone promotes pancreatic cancer cell death and reduction of tumor size through combined inhibition of histone deacetylation and induction of histone acetylation. Advanced in Preventive Medicine 2016;2016:1407840.
49. Salim LZA, Mohan S, Othman R, Abdelwahab SI, Kamalidehghan B, Sheikh BY, et al. Thymoquinone induces mitochondria-mediated apoptosis in acute lymphoblastic leukaemia in vitro. Molecules Journal .2013;18(9):11219-40.
50. Gali-Muhtasib H, Roessner A, Schneider-Stock R. Thymoquinone: a promising anticancer drug from natural sources. International Journal Biochemical Cell Biology. 2006;38(8):1249-53.
51. Park EJ, Chauhan AK, Min K-J, Park DC, Kwon T. Thymoquinone induces apoptosis through downregulation of c-FLIP and Bcl-2 in renal carcinoma Caki cells. Oncology Reports2016;36(4):2261-7.
52. Dastjerdi MN, Mehdiabady EM, Iranpour FG, Bahramian H. Effect of thymoquinone on P53 gene expression and consequence apoptosis in breast cancer cell line. International Journal of Preventive Medicine 2016;7.66.
53. Paramasivam A, Sambantham S, Shabnam J, Raghunandhakumar S, Anandan B, Rajiv R, et al. Anti-cancer effects of thymoquinone in mouse

neuroblastoma (Neuro-2a) cells through caspase-3 activation with down-regulation of XIAP. Toxicology Letters 2012;213(2):151-9.
54. Kundu J, Choi BY, Jeong C-H, Kundu JK, Chun K. Thymoquinone induces apoptosis in human colon cancer HCT116 cells through inactivation of STAT3 by blocking JAK2-and Src-mediated phosphorylation of EGF receptor tyrosine kinase. Oncology Report 2014;32(2):821-8.
55. Ke X, Zhao Y, Lu X, Wang Z, Liu Y, Ren M, et al. TQ inhibits hepatocellular carcinoma growth in vitro and in vivo via repression of Notch signaling. Oncotarget Journal 2015;6(32):32610.
56. Al-Rawashde FA, Taib WRW, Ismail I, Johan MF, Al-Wajeeh AS, Al-Jamal H. Thymoquinone Induces Downregulation of BCR-ABL/JAK/STAT Pathway and Apoptosis in K562 Leukemia Cells. Asian Journal Cancer Prevention 2021;22(12):3959.
57. El-Sayed SAE-S, Rizk MA, Yokoyama N, Igarashi IJP, vectors. Evaluation of the in vitro and in vivo inhibitory effect of thymoquinone on piroplasm parasites. Parasit Vectors 2019;12(1):1-10.
58. El-Mansy MN, Hassan MM, El-Nour A, Kholoud M, El-Hosary W. Evaluation the safety of thymoquinone loaded on gold nanoparticles in the treatment of hamster buccal carcinogenesis. Suez Canal University Medical Journal 2017;20(1):20-8.
59. Silvan S, Manoharan S. Apigenin prevents deregulation in the expression pattern of cell-proliferative, apoptotic, inflammatory and angiogenic markers during 7, 12-dimethylbenz [a] anthracene-induced hamster buccal pouch carcinogenesis. Archives of Oral Biology. 2013;58(1):94-101.
60. Dobbin ZC, Landen CN. Isolation and characterization of potential cancer stem cells from solid human tumors—potential applications. Current Protocol Pharmacology. 2013;63(1):14.28. 1-14.28. 19.